Lasers in Manufacturing Conference 2021

Striation formation at the cut edge of oxygen assisted fibre laser cutting

Handika Sandra Dewi[a,*]

[a]*Luleå University of Technology, Porsön, Luleå 971 87, Sweden*

Abstract

Laser cut edges show parallel grooves features or striations. A high-quality cut edge is identified by fine striations at the cut edge. In order to gain better understanding in striation formation at the cut edge and improve the cutting quality, striations at the cut edge and melt flow during laser cutting processes were investigated. Oxygen assisted fibre laser cutting processes were carried out on 1-mm-thick and 20-mm-thick steels at varied processing parameters and recorded using high speed imaging with borosilicate glass as replacement edge. The size of striations at the cut edge and frequency of the molten ripples were measured. The striation widths show a linear correlation with the gas pressure and cutting speed, but inverse correlation was found between striation widths and the nozzle diameter. Gas pressure is most likely the main influencing factor affecting the striation widths.

Keywords: gas density, pressure, fluid dynamics, steels;

1. Introduction

Laser cutting is a well-established manufacturing technique. The process involves focused laser beam to melt the materials and assisting gas to blow out the molten materials. Oxygen is the most common assist gas in laser cutting due to its ability in initiating exothermal reaction which adds energy to the process (Riveiro *et al.*, 2019). Although there is an increase trend of nitrogen usage in laser cutting, the oxygen laser cutting still offers the best cut edge quality in thicker specimens. Laser cut edge quality is determined by the striations mark on the cut edge surface where a good cut edge quality shows minimum striations mark on the cut edge surface.

The physical mechanisms of striation formation are currently of interest to improve the cut edge quality. Many investigators argue that striations patterns are due to an oscillated molten front during laser cutting process. There are two possible mechanisms that will result in an oscillated molten front: (1) the fluctuation of absorbed laser power during laser cutting and (2) the gas flow interacting with the work-piece will bring about fluctuation of the molten front (Schuöcker *et al.*, 2012). In special cases, the liquid layer can oscillate with a natural frequency even without fluctuations in absorbed power (Vicanek *et al.*, 1987). Additionally, the high-speed gas jet during melt ejection will cause hydrodynamic instabilities of the molten front.

Arata *et al.* suggested that when the cutting speeds are less than the velocity of the reactive front, the ignition and extinction cycles of reaction begin to take place (Arata *et al.,* 1979). However, a report indicate that although the cutting speed is above the critical speed, striations still exist (Ivarson *et al.*, 1994). Ivarson *et al.* then suggested a cyclic oxidation model. For diffusion-controlled reaction, the rate of chemical reaction is time dependent, being rapid in the early stages but decreasing markedly as the thickness of the oxide layer increases. Accordingly, the oxide layer will expand rapidly at first but slow down afterward. Once the oxide is blown out from the cutting front, another expansion will begin due to a sudden decrease of the oxide layer.

* Corresponding author.
E-mail address: contact@hsdewi.com .

Later on, Chen *et al.* investigated the mechanism of melt removal during laser cutting processes and found that the striation frequency is related to the frequency of the melt pool surface (Chen *et al.*, 1999). However, previous investigation on the cut edge of thick specimens showed that the striations appeared to be less apparent towards the bottom zone of the cut edge (Ivarson *et al.*, 2015). This result is not commonly found on the thin specimens. Since there is indication that mechanisms of melt ejection on thick specimens are different to the thin specimens, this work investigate laser cutting processes on 2 mm and 20 mm thick specimens to find the main influencing factors for striation formation during oxygen laser cutting processes.

2. Methods

2.1. Experimental set-up

Two sequences of oxygen assisted laser cutting experiment (Experiment A and B) were carried out using IPG Ytterbium fibre laser 1070 nm. Experiment A aimed to investigate cut kerf dynamics during oxygen laser cutting on a thick specimen, while Experiment B aimed to investigate influence of laser cutting parameters on the cut edge quality. Experiment A involved oxygen assisted laser cutting experiment on a 20 mm thick mild steel specimen observed using in situ high speed diagnosis technique (Arntz *et al.*, 2019). The technique employed borosilicate glass as a replacement edge allowing a direct view on the cut kerf during the process. A high speed imaging equipment and a continuous illumination laser were placed facing the specimen edge as shown in Figure 1(a). The laser beam was placed at the specimens' edge and moved along the positive X-axis. The edge quality of specimens cut using glass is comparable to the specimens cut under normal laser cutting condition. Accordingly, the dynamics seen through the glass can represent the dynamics during actual laser cutting condition. The high speed camera recorded the process at acquisition rate of 10,240 Hz.

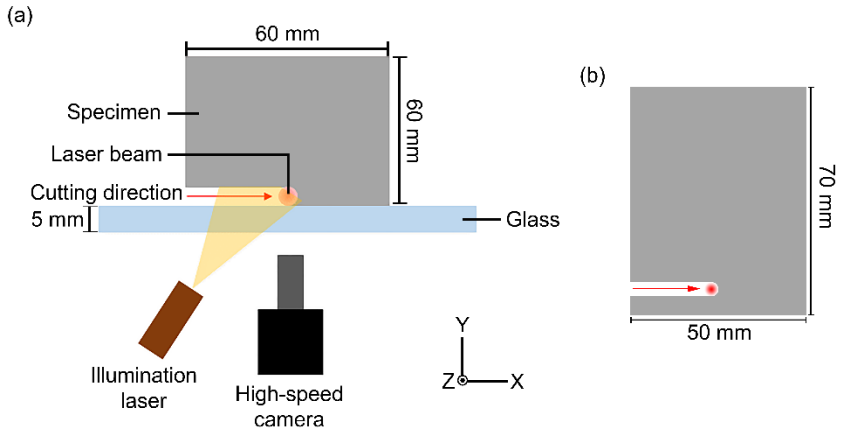

Figure 1. Illustration of the experimental set-up for oxygen assisted laser cutting processes on (a) a 20 mm thick specimen (Experiment A) and (b) 2 mm thick specimens (Experiment B).

Experiment B contained oxygen assisted laser cutting experiments on 2 mm thick mild steel specimens using variations of laser cutting parameters. High-speed imaging system was not used during Experiment B. The laser beam was placed approximately 10 mm behind the specimen edge and moved along positive X-axis as illustrated in Figure 1(b). Laser cutting parameters used in both Experiment A and B are available in Table 1.

Table 1. Laser cutting parameters used in both Experiment A and B

Parameters	Experiment A	Experiment B
Laser power (W)	4500	1200
Cutting speed (m/min)	0.7	60, 96, 120
Gas	Oxygen	Oxygen
Gas pressure (bar)	1.75	1.5, 2.5, 3
Nozzle diameter (mm)	1.5	1, 2, 2.5
Distance between nozzle and specimen surface (mm)	0.3	1, 1.5, 2

2.2. Analysis

Observation of the cut edge quality was carried out on specimens from both experimental sequences, while the cut kerf dynamics were observed using recorded high-speed video during Experiment A. Figure 2 illustrates the observation method for both cut edge quality and cut kerf dynamics. Striation lengths were measured from the start of dark feature to the end of bright feature on the macrograph images as illustrated by X in Figure 2(a). Consecutively, striation frequency were calculated as the inverse of striation length.

The cut kerf of 20 mm thick specimen was observed according to three zones (Top, Middle and Bottom) illustrated on Figure 2(b). Figure 2(b) shows a frame taken during Experiment A. The frame reveals an inclined cut front and melt pool direction during the process. The inclination angle was measured for each zone by comparing the cut front to the normal axis (θ), while the melt pool width was measure along the visible melt on the cut edge up to the cut front (M). Melt pool frequency is the amount of ripples seen along the melt pool at each zone divided by the distance of melt pool path (L).

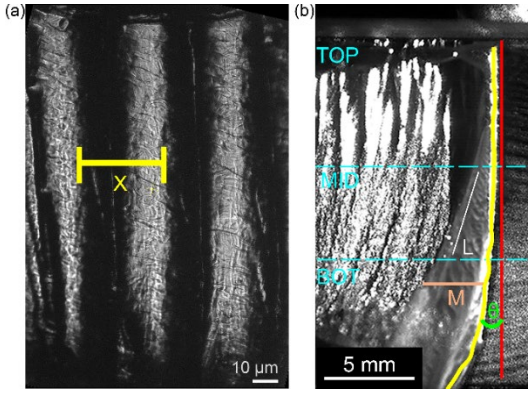

Figure 2. (a) Measurement of striation length on a cut edge and (b) cut kerf observation involving measurement of cut front inclination angle (θ), melt pool width (M) and length of melt pool pathway (L) at the top, middle and bottom zones of the 20 mm thick specimen.

3. Results

3.1. Macrograph pictures of the cut edge

Figure 3 shows comparison of cut edge from the 2 mm and 20 mm thick specimens. The 2 mm thick specimen shows deep parallel groove along the cut edge as seen in Figure 3(a). However, the 20 mm thick specimen shows the deep parallel grooves only at the top zone as seen in Figure 3(b). The grooves disappear and become less apparent towards the bottom zone that is appeared as striation-free cut edge.

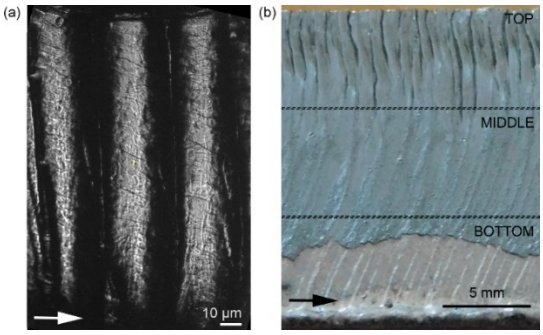

Figure 3. Appearance of striation on the (a) 2 mm thick specimen and (b) 20 mm thick specimen with arrows representing the cutting direction.

Figure 4 shows that changes in cutting speed, gas pressure, nozzle diameter and distance between nozzle and specimen surface influence the shape of striations on the cut edge. Change of nozzle diameter and gas pressure shows high influence on the striations width. The grooves become narrower as the nozzle diameter increased, while the opposite applies for changing the gas pressure.

3.2. Correlation between striation frequency and laser cutting parameters

Changes of nozzle diameter and gas pressure significantly influence the striation frequency as shown in Figure 5. This result agrees with previous observation on the cut edge micrographs. Striation frequency shows a linear correlation to the nozzle diameter (Figure 5(a)), but it shows an inverse correlation towards gas pressure (Figure 5(b)). However, the value of striation frequency tends to be constant for variations of cutting speed and distance between nozzle and specimen surface as shown in Figure 5(c) and (d).

3.3. Cut kerf dynamics

Figure 6(a) shows frames taken every 100 ms during Experiment A. The recorded frames show consistent melt pool shape at the top, middle and bottom zones. The melt pool width seen on the cut edge appear to be larger at the bottom zone, while the cut front inclination angle gradually increase from the middle zone to the bottom zone. Increase of melt pool width and cut front inclination angle is also shown in Figure 6(b) and (c). The melt pool width seen on the cut edge and cut front inclination angle is significantly higher at the bottom zone.

As previously observed on the cut edge micrograph, Figure 6(d) also shows that the middle and bottom zone show lower amount striation per mm compared to the top zone. However, observation on the melt ejection during the process shows that the middle zone has the highest amount of ripples on the melt per millimetre compared to the top and bottom zone (Figure 6(e)).

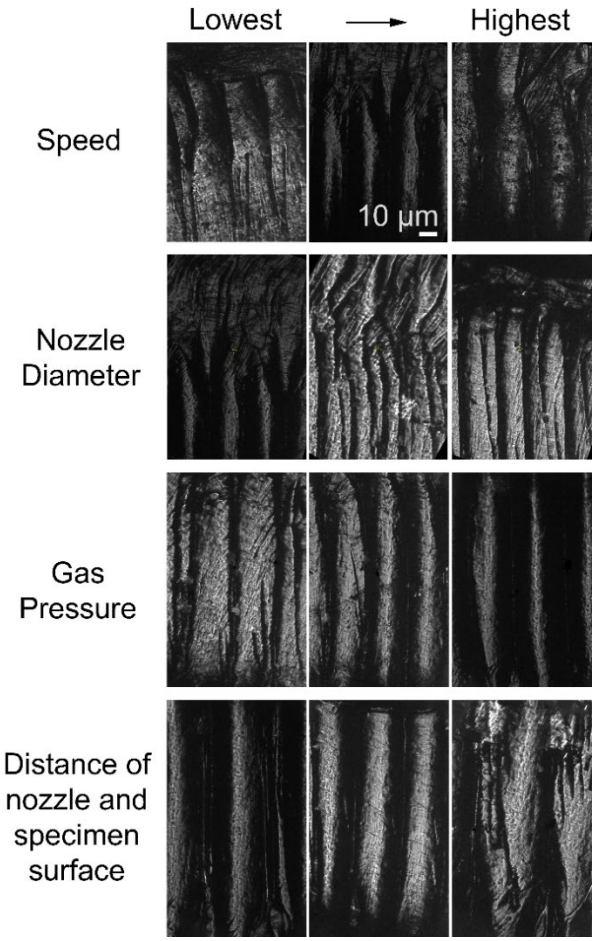

Figure 4. Cut edge quality of 2 mm thick specimens at variations of laser parameters with an arrow representing the cutting direction.

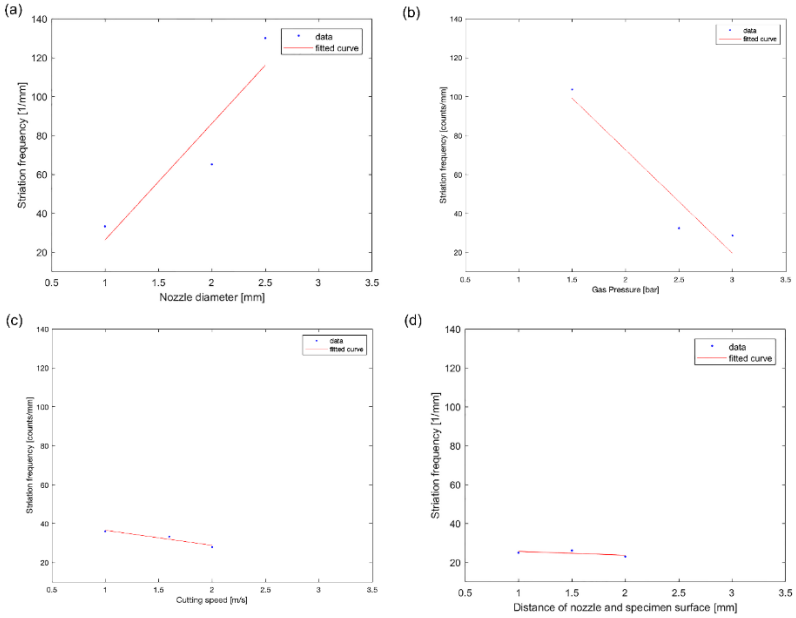

Figure 5. Correlation between striation frequencies and (a) nozzle diameter, (b) gas pressure, (c) cutting speed, (d) distance of nozzle and specimen surface.

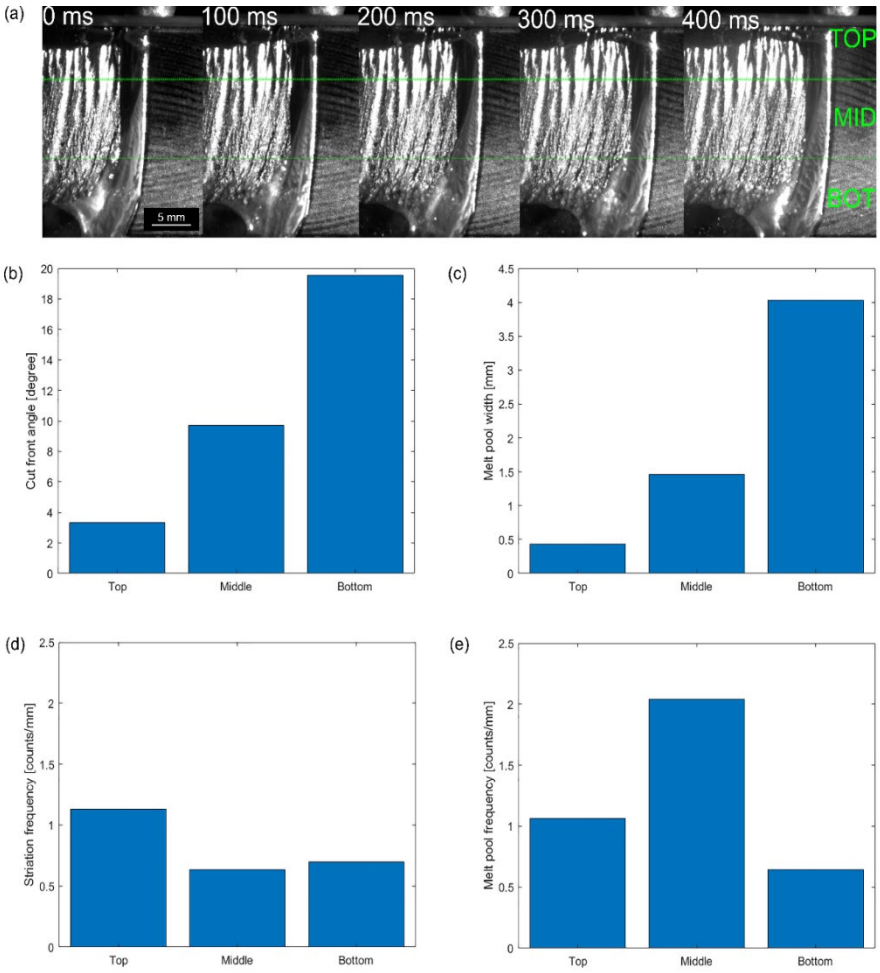

Figure 6. (a) Example of frames recorded by high-speed camera during Experiment A including measurement results for (b) cut front inclination angle, (c) melt pool width seen on the cut edge, (d) striation frequency on the cut edge and (e) melt pool frequency at the top, middle, and bottom zones of 20 mm thick specimen.

4. Discussion

There are three essential aspects from the results which will be discussed in the following passages. These aspects are (1) three distinguishable zones on the cut edge of 20 mm thick specimen, (2) significant influence of nozzle diameter and gas pressure to the cut edge quality, and (3) the correlation of striation frequency and melt pool frequency.

The striation frequency at the top zone of 20 mm thick specimen shows similar value to the melt pool frequency at the same zone. However, the melt pool frequency at the middle zone is doubled the value of striation frequency at the same zone. This indicates that there is no direct correlation between the striation frequency and melt pool frequency. Accordingly, there must be other influencing factors to consider which can influence the striation formation.

The 20 mm thick specimen shows different cut edge characteristics to the 2 mm thick specimen where the grooves become less apparent at the middle and bottom zones of the 20 mm thick specimen cut edge. Observation on the recorded high-speed video shows that the cut front inclination angle and melt pool seen on the cut edge increased at the middle and bottom zones. A high inclination angle at the bottom zone indicates that this zone experienced less energy input during the process compared to the top zone. Since the oxygen laser cutting process is driven by energy from the laser and exothermal reaction of Iron-Oxygen (Riveir*o et al*., 2019), the inclined cut front at the bottom zone can be related to the properties of the laser beam and local oxygen concentration. The bottom zone is located away from the laser beam focal position and nozzle opening. It means that the laser beam hitting this zone is defocused, while the oxygen content is reduced in this zone due to contamination of ambient air (Chen *et al.*, 1999). Accordingly, the bottom zone experience the least energy input from both the laser and exothermal reaction of Iron-Oxygen.

Low energy input impacts the melt pool behaviour at the bottom zones of the specimens. Low energy input can lead to a low temperature on the cut kerf. Since the energy input decreases towards the bottom zone, the temperature might also decrease towards the bottom zone. The top, middle, and bottom zones are most likely experiencing temperature gradients where the bottom zone possess the lowest temperature respectively. Low temperature leads to a high viscosity of molten steel (Hirai, 1993; Sato, 2011). As the temperature is decreasing towards the bottom zone, the viscosity of the molten materials is expected to increase at the bottom zone. Molten material with a high viscosity can have difficulties to flow away from the specimen and thus sticks on the cut edge causing a widening of the melt pool seen on the cut edge (Figure 6(a)). Additionally, momentum of the flowing gas can be lower at the bottom zone compare to the top zone as the bottom zone is away from the nozzle opening. Low flowing gas momentum can restrict the melt ejection, lowering the flow rate of molten metal and change its flow direction.

Increase of gas pressure causes decreased in striation frequency on the cut edge (Figure 5(b)). However, the macrograph pictures of the cut edge quality (Figure 4) shows that at a high gas pressure, the grooves appear wider and deeper compared to a low gas pressure. The gas pressure was measured at the oxygen tube used during the experiment. This means that the gas density (amount of oxygen molecules per volume) increased when the gas pressure was increased. High gas pressure then delivered large amount of oxygen molecules to the specimen which can increased the exothermal reaction during the process. Increased of exothermal reaction can cause high temperature in the cut kerf and lowering the viscosity of molten materials. Gas flow rate and momentum are also high when the gas pressure is high. These causes more material being removed and leaving wide and deep groove mark on the cut edge. In contrast, gas pressure was kept constant when nozzle diameter was varied. This means that the same amount of oxygen molecules were delivered to the specimens through varied cross-sectional volumes. Large nozzle diameter indicates large cross-sectional volume and thus lower oxygen density. Therefore, variation of nozzle diameter shows an inverse behaviour to the variation of gas pressure.

5. Conclusion

Since correlation of striation frequency and melt pool frequency was not found on the 20 mm thick specimen, the melt pool frequency is not likely to influence the striation frequency or cause striations on the cut edge.

Varied amount of oxygen molecules through varying gas pressure during the process influence temperature and viscosity of molten material. Additionally, gas pressure relates to the gas flow momentum which determines the melt flow ejection. Therefore, viscosity of the molten material together with momentum of the flowing gas seem to be the main influencing factor of the striation formation on the cut edge. Accordingly, variation of nozzle shape, such as rectangular, can reduce the striations on the cut edge.

Acknowledgment

The author gratefully acknowledge the funding from VINNOVA, Swedish Innovation Agency for the project ACCEL NO. 2019-00781_VINNOVA

References

Arata, Yoshiaki; Maruo, H. M. and Isamu; Takeuchi, S. (1979) 'Dynamic Behavior in Laser Gas Cutting of Mild Steel(Welding Physics, Processes & Instruments)'. Available at: http://hdl.handle.net/11094/10301.

Arntz, D. *et al.* (2019) ' In situ high speed diagnosis—A quantitative analysis of melt flow dynamics inside cutting kerfs during laser fusion cutting with 1 µ m wavelength ', *Journal of Laser Applications*, 31(2), p. 022206. doi: 10.2351/1.5096091.

Chen, K., Yao, Y. L. and Modi, V. (1999) 'Numerical simulation of oxidation effects in the laser cutting process', *International Journal of Advanced Manufacturing Technology*, 15(11), pp. 835–842. doi: 10.1007/s001700050140.

Hirai, M. (1993) 'Estimation of Viscosities of Liquid Alloys', *Isij International*, 33(2), pp. 251–258. doi: 10.2355/isijinternational.33.251.

Ivarson, A. *et al.* (1994) 'The oxidation dynamics of laser cutting of mild steel and the generation of striations on the cut edge', *Journal of Materials Processing Technology*, 40(3), pp. 359–374. doi: https://doi.org/10.1016/0924-0136(94)90461-8.

Ivarson, A., Powell, J. and Siltanen, J. (2015) 'Influence of Alloying Elements on the Laser Cutting Process', *Physics Procedia*. Elsevier B.V., 78, pp. 84–88. doi: 10.1016/j.phpro.2015.11.020.

Riveiro, A. *et al.* (2019) 'Laser Cutting: A Review on the Influence of Assist Gas', *Materials (Basel, Switzerland)*. MDPI, 12(1), p. 157. doi: 10.3390/ma12010157.

Sato, Y. (2011) 'Representation of the viscosity of molten alloy as a function of the composition and temperature', *Japanese Journal of Applied Physics*, 50(11 PART 2). doi: 10.1143/JJAP.50.11RD01.

Schuöcker, D., Aichinger, J. and Majer, R. (2012) 'Dynamic Phenomena in Laser Cutting and Process Performance', *Physics Procedia*, 39, pp. 179–185. doi: https://doi.org/10.1016/j.phpro.2012.10.028.

Vicanek, M. *et al.* (1987) 'Hydrodynamical instability of melt flow in laser cutting', *Journal of Physics D: Applied Physics*. IOP Publishing, 20(1), pp. 140–145. doi: 10.1088/0022-3727/20/1/021.